Geogr. Fis. Dinam. Quat.
38 (2015), 67-78, 13 figg., 5 tab.

DOI 10.4461/GFDQ.2015.38.07

PETR SKLENÁŘ(*), ANDREA KUČEROVÁ(**), JANA MACKOVÁ(***) & PETR MACEK(****)

TEMPORAL VARIATION OF CLIMATE IN THE HIGH-ELEVATION PÁRAMO OF ANTISANA, ECUADOR

ABSTRACT: SKLENÁŘ P., KUČEROVÁ A., MACKOVÁ J. & MACEK P., *Temporal variation of climate in the high-elevation páramo of Antisana, Ecuador.* (IT ISSN 0391-9838, 2015).

We monitored the climate in high-elevation páramo of Antisana (Ecuador) to analyze its diurnal and annual variation. We established two climatic stations on the western (leeward) side of the mountain at 4280 m and 4600 m, and two stations on the north-eastern (windward) side at 4120 m and 4430 m. We recorded air temperature at 100 cm above ground, relative air humidity, and global solar radiation in hourly intervals from July 2007 to December 2010. Moreover, we recorded precipitation at the two lower stations. The western side received 1098 mm of rainfall per year with two maxima in April–June and October–November. In contrast, the north-eastern side received 2694 mm with a single maximum in June. The air was almost permanently saturated with moisture, both during the day and the year, on the north-eastern side with mean relative air humidity of 98%. On the western side, the air humidity showed distinct daily and seasonal variation; it dropped to 80% at noon and had two annual minima in January and September. The western side of Antisana received 35% more solar radiation than the north-eastern side. Furthermore, the mostly cloudy weather on the north-eastern side tended to eliminate the mid-day maximum of radiation. The stations at higher elevations received 11% more solar radiation than the stations at lower elevations and experienced a more distinct seasonal variation with the maximum during August–September. Mean annual air temperature varied within 2K at all stations, which contrasted with the mean daily oscillation of 8–10K on the western side and 5K on the north-eastern side. Night frosts were frequent on the western side whereas high humidity and cloudiness on the north-eastern side reduced the number of frost nights. Frosts were rather mild and of short duration; the minimum temperature recorded was –6.1°C and most frost periods lasted less than four hours. Freezing temperatures were most frequent during periods of reduced humidity. Temperature lapse rates calculated for the 300 m elevational gradient were 0.44 K/100 m and 0.55 K/100 m for the western and north-eastern sides, respectively. Potential evapotranspiration values suggested that water was in surplus year-round on the north-eastern side of Antisana, but its availability was limited during drier periods on the western side.

KEY WORDS: Equatorial Andes, Mountain climate, Seasonality, Superpáramo, Tropical alpine environment.

RESUMEN: SKLENÁŘ P., KUČEROVÁ A., MACKOVÁ J. & MACEK P., *Variación temporal del clima en el páramo de Antisana, Ecuador*. (IT ISSN 0391-9838, 2015).

La variación diaria y anual del clima se estudió en el páramo de Antisana (Ecuador) en dos estaciones climáticas localizadas en el lado occidental de la montaña a alturas de 4280 m s.n.m. y 4600 m s.n.m. y en dos estaciones localizadas en el lado nor-oriental a alturas de 4120 msnm y 4430 msnm. La temperatura del aire a 100 cm por encima del suelo, la humedad relativa del aire y la radiación global de sol se registraron de manera continua cada hora desde julio 2007 hasta diciembre 2010. La precipitación se registró en las dos estaciones de alturas bajas. El promedio anual de precipitaciones fue 1098 mm en el lado occidental con épocas mas húmedas en abril–junio y octubre–noviembre. Por el contrario, en el lado nor-oriental el promedio anual fue 2694 mm con junio cómo el mes más húmedo. En el lado nor-oriental la humedad relativa del aire permaneicó muy alta casi todo el tiempo con un valor promedio de 98%. En el lado occidental la humedad relativa mostró un ritmo diario y annual; la humedad bajó hasta 80% en el mediodía y mostró dos minimos anuales en enero a septiembre. El lado occidental recibió un 35% más de radiación solar que el lado nor-oriental. Las dos estaciones de alturas altas recibierón un 11% más de radiación que las dos estaciones de alturas bajas y mostrarón una variación anual distinta con máximos en agosto–septiembre. La variabilidad interanual de la temperatura del aire no alcanzó 2K en ninguna de las estaciones, por el contrario, el promedio de las oscilaciones diarias fue 8–10K en el lado occidental y 5K en el lado nor-oriental. En el lado occidental se registraron frecuentemente temperaturas nocturnas bajo 0°C mientras que en el lado nor-oriental la frecuencia de días con heladas fue reducida por la alta

(*), *Department of Botany, Charles University, Benátská 2, 128 01 Prague, Czech Republic*

(**), *Institute of Botany, Czech Academy of Sciences, Dukelská 135, 379 82 Třeboň, Czech Republic*

(***), *Institute of Soil Biology, Biology centre, Czech Academy of Sciences, Na Sádkách 7, 370 05 České Budějovice, Czech Republic*

(****), *Faculty of Science, University of South Bohemia, Branišovská 31, 370 05 České Budějovice, Czech Republic*

The study was supported by the Grant Agency of the Academy of Sciences, Czech Republic (IAA601110702), by the long-term research development project no. RVO 67985939, and partly also by the Ministry of Education of the Czech Republic (MŠMT 0021620828). PM was additionally supported by CzechPolar grant LM2010009. An anonymous reviewer is acknowledged for insightful comments on the earlier draft of the manuscript. Katya Romoleroux and Hugo Navarrete (PUCE, Quito) are thanked for providing research facilities in Ecuador, Luis Maisincho (INAMHI, Quito) is thanked for providing access to the Antizana15 climatic data for comparison, and Ministerio del Ambiente and señor José Delgado are acknowledged for research and entry permits, respectively. Keith Edwards kindly provided linguistic revision.

humedad y nubosidad. En general, las noches con heladas fueron moderadas (la temperatura mínima registrada fue –6.1°C) y la duración de temperaturas bajo 0°C fue corta (menos de cuatro horas). Temperaturas bajo 0°C ocurrierón más frecuentemente en periodos con la humedad reducida. El gradiente térmico altitudinal fue 0.44 K/100 m en el lado occidental y 0.55 K/100 m en el lado nor-oriental. Según los valores de evapotranspiración potencial, en el lado nor-oriental siempre hubo exceso de agua mientras que en el lado occidental hubo escasez de agua durante los periodos secos.

PALABRAS CLAVES: Ambiente alpino tropical, Andes ecuatoriales, Clima de montaña, Estacionalidad, Superpáramo.

INTRODUCTION

The warm and humid climate of the lowland tropics along with the seasonal climate with warm summers and cold winters of the temperate–to–arctic zones are the norm for vast geographic areas. In contrast, the tropical alpine climate is one of the most specific climates on Earth, which is encountered only on the highest equatorial mountains (Sarmiento, 1986; Barry, 2008). General features of the tropical alpine climate are well-known – it is most characteristically described by a pronounced daily temperature oscillation along with frequent night frosts throughout the year (Troll, 1968; Sarmiento, 1986; Rundel, 1994). Precipitation, in contrast to temperature, is distributed more unevenly both during the year due to annual patterns of atmospheric circulation and between years due to e.g., ENSO events (Bendix & Lauer, 1992; Vuille & *alii*, 2000a, b). Precipitation occurs mainly in the form of rainfall, although the highest elevations experience snow and hail (Sarmiento, 1986; Bendix & Rafiqpoor, 2001; Jomelli & *alii*, 2009).

Knowledge about the climate of the tropical high Andes, i.e., páramo, is often derived from short-term climatic records spanning several days or weeks (e.g., Diemer, 1996; Sømme & *alii*, 1996; Sklenář, 1999). Climatic measurements lasting longer than one year are uncommon and especially the highest elevations are insufficiently covered (Vuille & *alii*, 2008). Long-term climatic observations are available from the mid-elevations of the páramo belt (Azócar & Monasterio, 1980; Anonymous, 1978–1990; Jørgensen & Ulloa, 1994) and sometimes data are gathered from the vicinity of glaciers (e.g., Wagnon & *alii*, 2009). The most complex climatic data representative of the entire páramo belt were provided by the ECOANDES project in the Central Cordillera of Colombia (Javellas & Thouret, 1995; van der Hammen & *alii*, 1995; Witte, 1995).

In tropical alpine environments, the daily temperature variation greatly surpasses the seasonal variation and so the climate is often paraphrased as "summer every day, winter every night" (Hedberg 1964). In contrast to this common knowledge about the temperature course, patterns of daily versus seasonal variation of other climatic variables have been addressed less frequently (e.g., Azócar & Monasterio, 1980). Yet the annual climatic variation is important in determining e.g., phenology of tropical alpine biota, although causal mechanisms usually remain poorly understood (Kudo & Suzuki, 2004; Fagua & Gonzalez, 2007). Moreover, long-term climatic measurements from the upper páramo belt of the humid equatorial Andes are virtually lacking. We thus established microclimatic stations on the slopes of the Antisana volcano in Ecuador to monitor variation of the high-elevation páramo climate. In this paper, we describe the patterns and quantify the temporal variation of air temperature, solar radiation, air humidity, precipitation, and potential evapotranspiration using data from three years of observations. In particular, we examined how much the daily and seasonal variation in temperatures are mirrored by variation of other climatic variables.

METHODS

STUDY SITE

The study was carried out on the slopes of Antisana (5704 m; 0°30'S 78°10'W), which is a mountain located in the eastern cordillera of Ecuador. Glaciers crown the top of Antisana and reach as far down as 4800 m and 4600 m on the western and eastern sides, respectively. However, older moraines indicate earlier glaciers about 1200 m lower (Hastenrath, 1981; Clapperton & *alii*, 1997; Rabatel & *alii*, 2013). Antisana is considered an extinct volcano, although the latest activity dated to the beginning of the 19th century (Sauer, 1971; Hall, 1977). A high-elevation plateau (between 4000 – 4200 m) is present on the south-western side of the mountain (fig. 1) and is mostly covered by grass páramo vegetation.

Antisana hosts a diverse páramo flora and distinct types of vegetation (Sklenář & Lægaard, 2003; Sklenář & *alii*, 2008). On the eastern (windward) side, sclerophyllous shrubs (*Loricaria*, *Diplostephium*) share dominance with cushion plants (*Azorella*, *Plantago*, and *Werneria*), and locally also with bamboo and tussock grasses (*Neurolepis*, *Calamagrostis*, *Festuca*) at lower elevations. At higher elevations, prostrate subshrubs (*Disterigma*, *Pernettya*) along with herbs and small grasses (e.g., *Lachemilla*, *Oritrophium*,

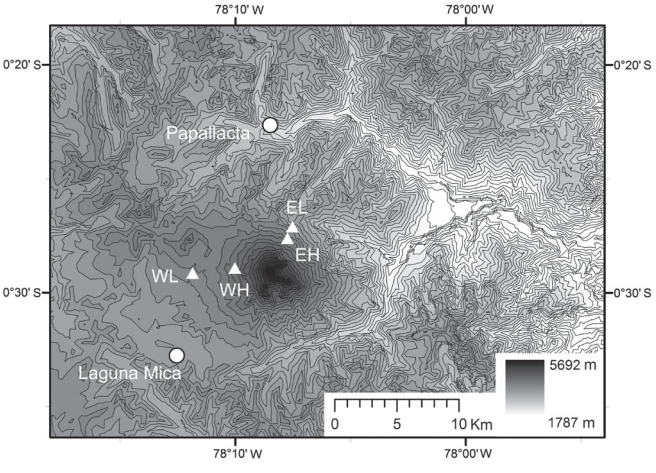

FIG. 1 - Topography map of the Antisana volcano with location of the four climatic stations; contour lines are in 100 m intervals; WL means western lower site, WH means western higher site, EL means north-eastern lower site, and EH means north-eastern higher site.

TABLE 1 - Geographic location, instrumentation, and period of operation of the four microclimatic stations on the slopes of the Antisana volcano.

Locations		**Western lower**	**Western higher**	**North-eastern lower**	**North-eastern higher**
Elevation		4280 m	4600 m	4120 m	4430 m
Latitude		00°29'09"	00°28'55"	00°27'06"	00°27'37"
Longitude		78°11'52"	78°10'02"	78°07'32"	78°07'45"
Instrument	**Position**	**Period of operation**	**Period of operation**	**Period of operation**	**Period of operation**
Precipitation, 8" Raingauge 372C, MetOne, Oregon, USA + MicroLog datalogger, EMS Brno	100 cm	Jul 2007–Dec 2010	NA	14 Aug–30 Sep 2007, 3 Nov 2007–29 Feb 2008, 16 Jul–21 Oct 2008, 18 Mar–9 Dec 2010	NA
Air temperature, Pt100 sensor + Minikin datalogger, EMS Brno	100 cm	Jul 2007–Dec 2010	Jul 2007–Dec 2010	Jul 2007–Jan 2010	Jul 2007–Jun 2008
Global radiation, sensor EMS 11 + Minikin dataloger, EMS Brno	100 cm	Jul 2007–Nov 2010, missing Aug–Oct 2009	Jul 2007–Nov 2010	Jul 2007–Nov 2010, missing Jul 2008	Jul 2007– Nov 2010, missing Jun–Jul 2008
Relative air humidity, sensor EMS 33 + Minikin datalogger, EMS Brno	100 cm	Jul 2007–Dec 2010	Jul 2007–Dec 2010	Jul 2007–Jan 2010	Jul 2007–Jun 2008

Agrostis) are common. On the western (leeward) side, tussocks of *Calamagrostis* grasses are abundant at lower elevations along with sclerophyllous shrubs (*Chuquiraga*), rosulate herbs (*Valeriana*, *Werneria*), and prostrate subshrubs (*Baccharis*, *Lupinus*). This vegetation gives way to patchy upper superpáramo vegetation of small herbs and grasses (Black, 1982; Sklenář, 2000). Cushion-bogs occur along streams and in terrain depressions.

The region was declared an ecological reserve, Reserva Ecológica Antisana, in 1993 in order to protect vast reaches of montane forest and páramo. In spite of that, the páramo on the western side of the mountain is heavily grazed by cattle and sheep which commonly results in severe degradation of the soil and vegetation (Grubb, 1970; Black, 1982; Sklenář, 2000).

Data acquisition and treatment

Four microclimatic stations were established on two opposite sides of the Antisana volcano in July 2007 (fig. 1; tab. 1) and operated until December 2010. Two stations were located on the western side at 4280 m and 4600 m, and two stations were located on the north-eastern side at 4120 m and 4430 m. The roughly 200 m shift in the elevational position of the stations between the western and eastern sides reflected the climatic asymmetry of the equatorial Andes (Troll, 1968; Lauer, 1979), so that the stations on the opposite sides thus occurred in corresponding vegetation types (Sklenář, 2000; Sklenář & Lægaard, 2003). The two lower sites corresponded to the transition between the grass (western side) and bamboo (north-eastern side) páramo vegetation to lower superpáramo vegetation and were characterized by closed (or almost so) plant cover. The two higher sites were located in the sparsely vegetated upper superpáramo (e.g., Sklenář, 2006).

All stations were established in open areas of the páramo, i.e., they were unobstructed by any tall vegetation, rocks, etc. The stations were equipped with a set of dataloggers with built-in sensors to record incident global radiation (Rg), air temperature (T100), and relative air humidity (RH) (tab. 1). The Rg, T100, and RH sensors and loggers were screened by white radiation shields and were positioned on aluminum poles at 100 cm height above ground; due to technical limitations, the temperature sensors were not actively ventilated. The sensors and dataloggers were supplied by EMS Brno, Czech Republic (www.emsbrno.cz). The stations at lower elevations were equipped with automated Model 372 precipitation gauges with funnel diameter of 20.3 cm designed to measure rain and snow. The gauges, supplied by MetOne, Wisconsin, USA (www.metone.com), were placed on aluminum frames at 100 cm height above ground.

Measurements were taken from 26 July 2007 to 9 December 2010. The recording interval was set at 1 hour in all dataloggers except the rain gauges. Records were not complete for all variables due to damage of the sensors and/or dataloggers (tab. 1). Whereas the rain gauge recorded continuously during the entire period on the western side, the instrument on the north-eastern side operated only periodically, which yielded four common periods of rainfall measurements (14 August–30 September 2007, 3 November 2007–29 February 2008, 16 July–21 October 2008, 18 March 2009–9 December 2010).

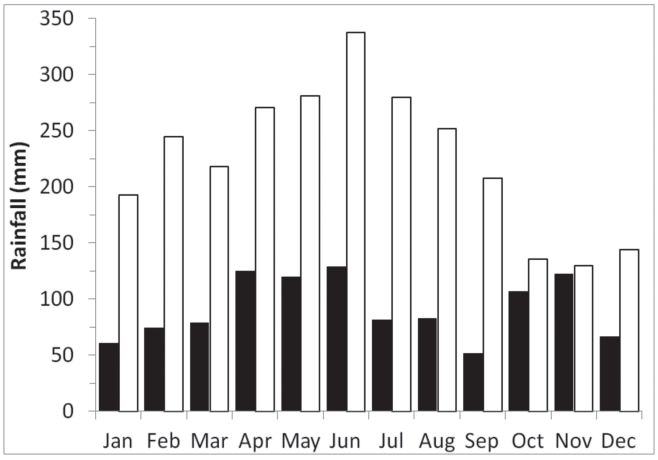

FIG. 2 - The seasonal course of precipitation in the páramo of Antisana measured on the western (black) and north-eastern (white) sides of the volcano during 2007–2010; mean annual sum of rainfall equals 1098 mm and 2694 mm, respectively.

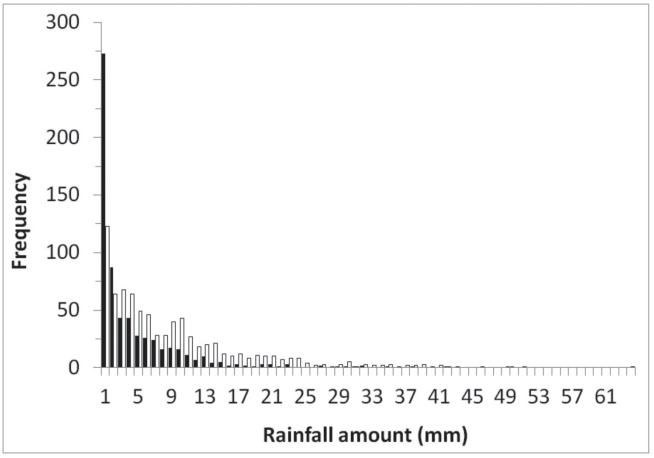

FIG. 3 - Frequency distribution of 24-hours rainfall sums on the western (black) and north-eastern (white) sides of the Antisana volcano during four overlapping measurement periods between August 2007 and December 2010 (see text for details). The distribution median equals 1.6 mm (western side) and 5.4 mm (north-eastern side), and the number of rainfall days are 639 (western side) and 781 (north-eastern side).

Potential evapotranspiration was calculated from Rg, RH and T100 using the Penman-Monteith method (Allen & *alii*, 1998). The calculations followed the Equation 1:

$$Et_o = \frac{0{,}408\ D\ (R_n - G) + g\ (900 / T + 273)\ U_2\ (e_a - e_d)}{+\ \gamma\ (1 + 0{,}34\ U_2)} \quad \text{Eq. 1.}$$

in which Et_o = evapotranspiration [mm .day^{-1}], R_n = net radiation [MJ m^{-2}day^{-1}], G = soil heat flux [MJ m^{-2}day^{-1}], T = mean daily temperature [°C], U_2 = wind speed at 2 m height [ms^{-1}], $e_a - e_d$ = the water vapour saturation deficit, and D = the slope of the saturation vapor pressure [kPa °C^{-1}], while 900 is a conversion factor.

Et_o describes the potential evapotranspiration from a water-saturated lawn. The soil heat flux was considered close to zero in a daily budget and was thus omitted. The equation includes an empirical dependence on wind speed. Since wind measurements could not be taken due to limited instrumentation, we used the value of 2 ms^{-1} for the whole data set as an approximation of low wind speed, following the FAO recommendation.

The daily and annual variation in climatic variables was compared by means of the coefficient of variation, which was calculated from hourly and monthly means or sums (where appropriate), respectively.

RESULTS

PRECIPITATION

Rainfall was distributed bimodally on the western side of the Antisana volcano with the main maximum in April–June and a secondary maximum in October–November with a mean annual sum of 1098 mm (due to incomplete records in December 2010, sums for the years were calculated for the continuous period December 2007–November 2010). The precipitation varied from 1050 mm in 2008 to 781 mm in 2009, and 1465 mm in 2010. The north-eastern side of the mountain had a unimodal distribution of rainfall with the maximum in June and the minimum in October–December (fig. 2) with a mean annual sum of 2694 mm. Although the records were incomplete in the first half of the measuring period, this estimate seems to be unbiased since there was 2626 mm of precipitation over the 12-month continuous record of December 2009–November 2010. Overall, 2562 mm of precipitation fell on the western side and 6594 mm on the north-eastern side, during the period of common measurements, which totaled 28 months. Individual time periods had the respective values of 64 mm and 341 mm (14 August–30 September 2007), 248 mm and 804 mm (3 November 2007–29 February 2008), and 247 mm and 916 mm (16 July–21 October 2008), and 2002 mm and 4533 mm (18 March 2009–9 December 2010) for the western and north-eastern sides, respectively.

Precipitation was distributed more evenly during the year on the north-eastern side of the Antisana volcano, varying by 33% (the value is a coefficient of variation calculated from monthly sums, n = 26), in contrast to 57% variation on the western side (n = 40). There were 639 days with rain on the western side compared to 781 rainy days on the north-eastern side, meaning that about 28% and 12% of days were without measurable precipitation, respectively. Although the absolute 24-hour maxima did not differ remarkably between the two sides, i.e., being 49.4 mm on the western and 63.2 mm on the north-eastern side (both values were recorded in the first half of 2010), rain fell in distinctly smaller amounts on the western side (fig. 3). Whereas more than 42% of rainy days yielded less than 1 mm of rain on

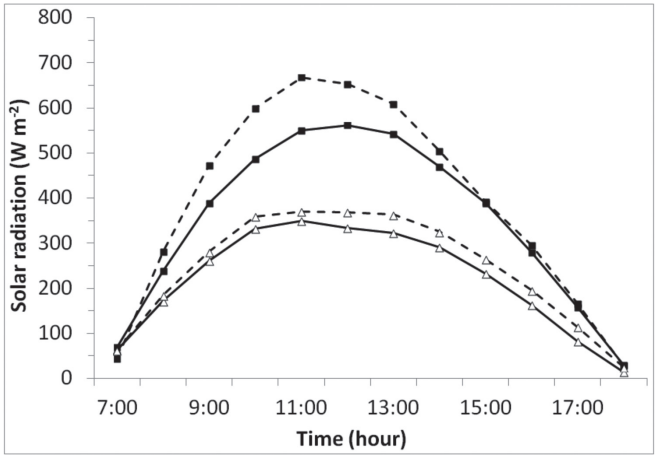

FIG. 4 - Daily course of solar radiation at the western lower (squares and solid curve), western higher (squares and dashed curve), north-eastern lower (triangles and solid curve), and north-eastern higher (triangles and dashed curve) climatic stations; values are means of hourly radiation.

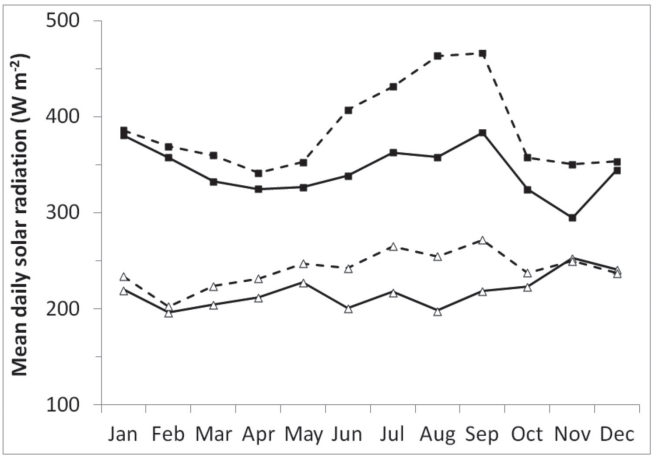

FIG. 5 - Seasonal course of mean daily solar radiation at the western lower (squares and solid curve), western higher (squares and dashed curve), north-eastern lower (triangles and solid curve), and north-eastern higher (triangles and dashed curve) climatic stations.

the western side, such small amounts occurred only in about 16% of rainy days on the north-eastern side. As a result, the median of the daily rainfall sums for the two sides was 1.6 mm and 5.4 mm, respectively.

SOLAR RADIATION

The daily mean value of solar radiation on the western side of the Antisana volcano was 346 ± 123.9 Wm^{-2} at the lower site and 387 ± 138.1 Wm^{-2} at the higher site, while respective values for the north-eastern side were 218 ± 101.9 Wm^{-2} and 243 ± 93.1 Wm^{-2}. Along with the major difference in the radiation values between the opposite mountain sides and a minor difference due to elevation, there was a distinct variation in temporal patterns among the sites. A mid-day peak of incident solar radiation can be seen on the western side, although the maximum seems to be shifted to 11:00 at the higher site in contrast to the lower site. On the north-eastern side, however, no distinct daily maximum was seen with almost constant values between 10:00 and 13:00 (fig. 4). Furthermore, solar radiation peaked in July–September on the western higher site with a similar, albeit much less distinct, increase at the lower site (fig. 5). As a result, the seasonal variation of incoming radiation was 11.6% at the higher site whereas it was only 7.5% at the lower site. A secondary peak in solar radiation was observed in December–January at both western sites. Such seasonal variation was essentially lacking on the north-eastern side being between 7.7–7.8% for the two sites, although slightly higher values occurred at the higher site during July–September.

AIR TEMPERATURE

The mean daily maximum surpassed 9°C at the western lower site while the mean night minimum dropped below zero yielding a mean daily oscillation of about 10K. In contrast, the mean daily range was about 5K on the north-eastern side (tab. 2). These differences in the daily range of air temperature between the two sides of Antisana were consistently present throughout the entire year, i.e., the western sites always experienced greater temperature oscillations. Air temperature peaked at noon on the western side, but the temperatures were rather constant and without a distinct maximum on the north-eastern side (fig. 6). The day-time climate was thus cooler on the north-eastern side as the summed hour-degrees (7:00–18:00) yielded values of 58.2 and 37.4 at the lower and higher sites, respectively, compared to 74.6 and 48.3 at the respective western sites. On the other hand, the climate on the north-eastern side was milder during the night compared to the western side, providing re-

TABLE 2 - Means and extreme values of air temperature measured at 100 cm above ground.

Station	Number of records	Absolute minimum (°C)	Mean daily minimum (°C)	Mean (°C)	Mean daily maximum (°C)	Absolute maximum (°C)
Western 4280 m	29785	-6.1	-0.5	3.7	9.6	15.0
Western 4600 m	29537	-4.1	-0.7	2.3	6.9	13.0
North-eastern 4120 m	29124	-3.1	1.6	3.8	6.6	14.3
North-eastern 4430 m	9176	-2.5	0.2	2.1	4.9	10.5

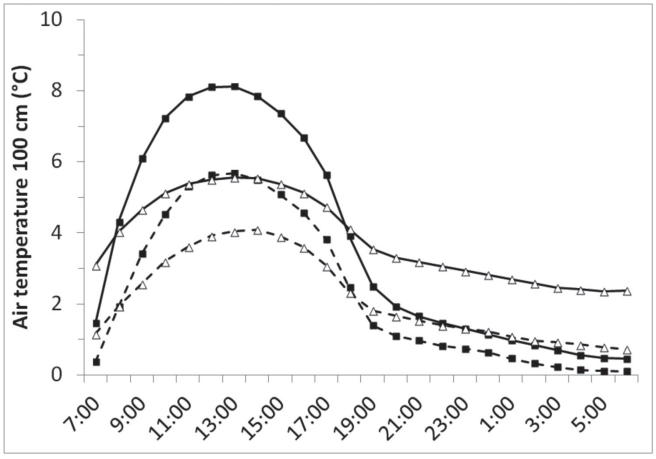

FIG. 6 - Daily course of mean air temperatures at 100 cm above ground at the western lower (squares and solid curve), western higher (squares and dashed curve), north-eastern lower (triangles and solid curve), and north-eastern higher (triangles and dashed curve) climatic stations.

spectively 33.7 hour-degrees and 14.0 hour-degrees for the north-eastern and western lower sites, and 14.3 hour-degrees and 7.1 hour-degrees for the north-eastern and western higher sites. In general, night frosts were mild at all sites and particularly on the north-eastern side of the mountain where the air temperature never dropped below –4°C (fig. 7); night air temperatures below –4°C occurred at a frequency of 1.3% at the western lower site and of 0.2% at the western higher site. The lowest air temperature of –6.1°C measured at 100 cm height was recorded at the western lower site.

Whereas the western side of the Antisana volcano was more variable on a daily basis, the variation during the year tended to be greater on the north-eastern side. Monthly mean air temperatures varied between 1.5–1.8K at the north-eastern sites, which corresponded to a relative yearly variation of 15–23%, whereas the variation was between 1–1.3K (~11–12%) at the western sites (fig. 7). Mean daily maximum temperatures varied between 2.1–3.2K (~13–14%) on the north-eastern side in contrast to 1.6–2K (~7%) on the western side, and similar patterns were seen for the absolute

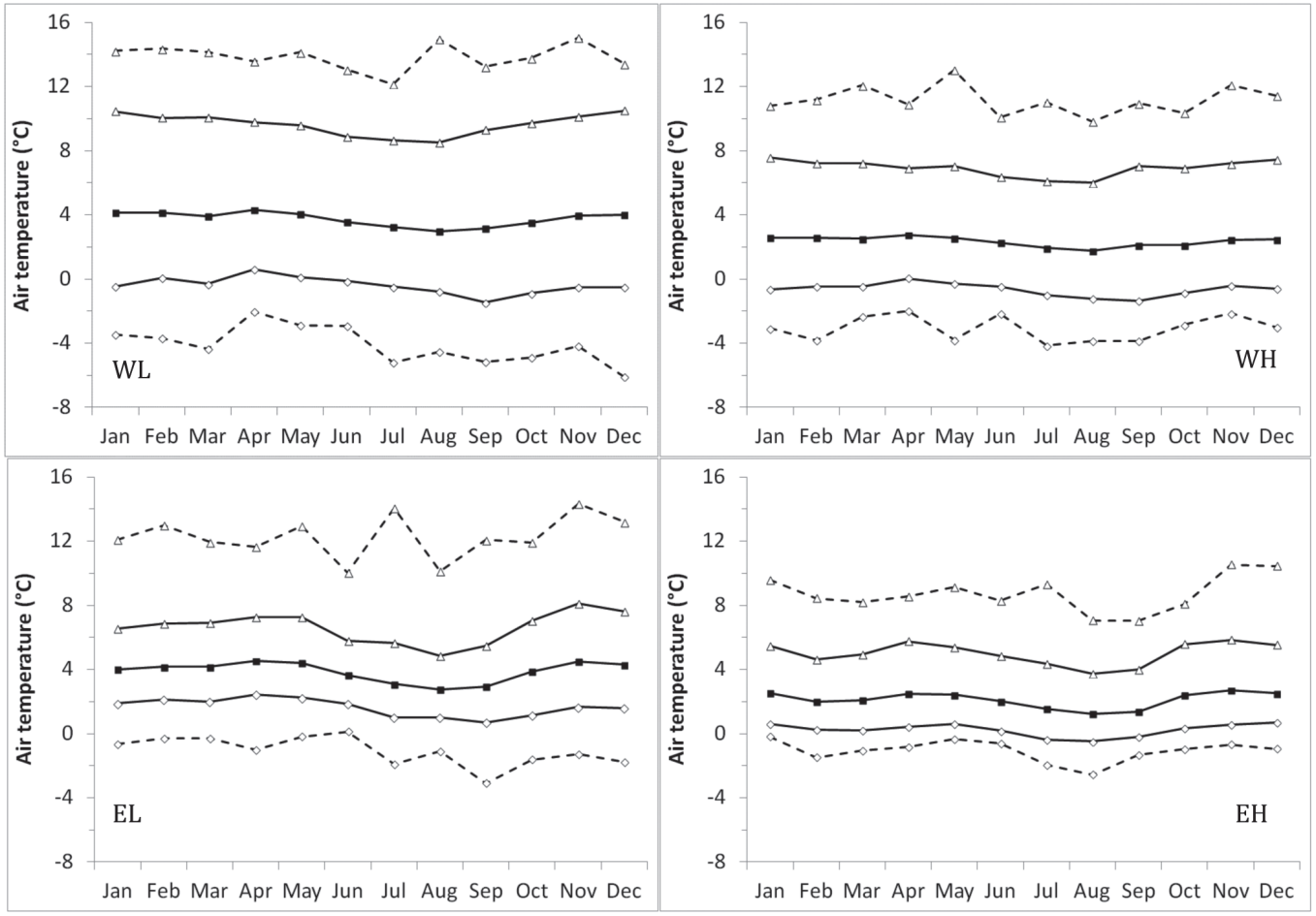

FIG. 7 - Seasonal variation of (from the bottom in each graph) the absolute minimum (diamonds, dashed line), mean minimum (diamonds, full line), mean (squares, full line), mean maximum (triangles, full line), and the absolute maximum (triangles, dashed line) air temperatures measured during the month at 100 cm above ground at the western lower (above left), western higher (above right), north-eastern lower (below left), and north-eastern higher (below right) climatic stations.

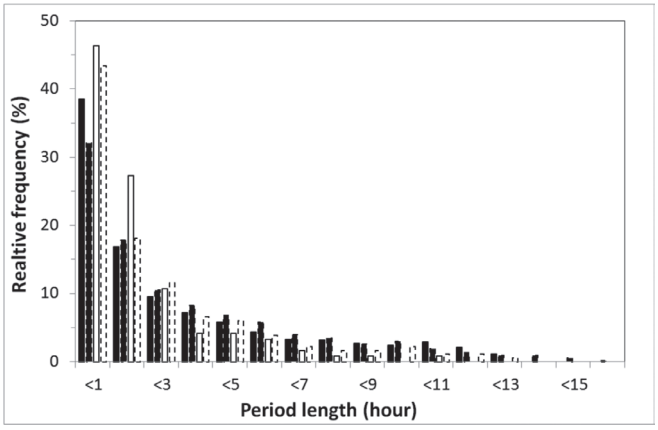

FIG. 8 - Relative frequency of freezing period duration at 100 cm above ground during the night (19:00–6:00) expressed as the number of consecutive measurement periods with temperatures below zero (i.e., one period ~ 1 hour) at the western lower (black columns, solid outline; n = 16125 records), western higher (black columns, dashed outline; n = 16006), north-eastern lower (white columns, solid outline; n = 14775), and north-eastern higher (white columns, dashed outline; n = 9203) climatic stations.

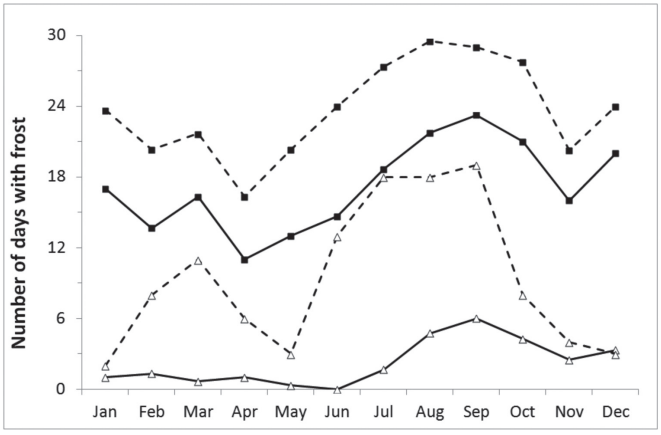

FIG. 9 - Number of days per month with air temperatures at 100 cm above ground falling below zero at the western lower (squares and solid curve), western higher (squares and dashed curve), north-eastern lower (triangles and solid curve), and north-eastern higher (triangles and dashed curve) climatic stations.

daily maxima and absolute night minima. Only the seasonal mean night minimum temperature tended to vary more at the western sites (1.4–2.1K corresponding to ~51–56% of relative variation) than at the north-eastern sites (1.2–1.7K, ~32–52%).

No day with permanent frost, i.e., with temperatures below zero during the entire 24 hours, was recorded at any site. The longest freezing period of 16 hours was observed twice at the western higher site. Except for the north-eastern lower site, freezing periods lasting the whole night, i.e., 12 consecutive hours, were occasionally observed (fig. 8). But in most cases, i.e., more than 75% of days on the western side and more than 85% of days on the north-eastern side, continuous freezing temperatures lasted less than four hours. Mean daily air temperature below zero was observed on less than 1% of days at the two higher sites, and there was a single such day at the western lower site. The occurrence of frost days had a distinct seasonal pattern with the maximum frequency during July–October at all sites (fig. 9). However, the number of frost days varied significantly among the sites. Whereas there were 29 frost days at the western higher site in September, the north-eastern lower site experienced only 6 such days. Although the number of freezing days at the north-eastern higher site significantly increased during September, the frosts were nevertheless mild and temperatures only rarely dropped below –1°C.

RELATIVE AIR HUMIDITY

The air was almost permanently saturated by water vapor on the north-eastern side of the Antisana volcano (tab. 3; figs. 10 and 11). As a result, mean air humidity was about 98% at both sites and varied by less than 1% during the day, although exceptionally values dropped as low as 20%. Essentially the same pattern was seen during the entire year as the seasonal variation in RH was only 0.6–0.8% for these two sites. In contrast, the RH fluctuated more on the western side both on a daily (4.6–8.2%) and seasonal (1.6–2.9%) basis. The air humidity still remained relatively high for most of the time with mean values between 90–92% (tab. 3). But since RH was largely determined by air temperature (correlation coefficients between RH and temperature, r = 0.733 and r = 0.512 for the two western sites), air humidity declined from the morning towards noon and rose in the late afternoon (fig. 10). Whereas air saturation by water vapor remained close to 100% at the

TABLE 3 - Means and extreme values of relative air humidity measured at 100 cm above ground.

Station	Number of records	Absolute minimum (%)	Mean daily minimum (%)	Mean (%)	Mean daily maximum (%)	Absolute maximum (%)
Western 4280 m	29231	17.9	69.8	91.8	99.9	100
Western 4600 m	29517	10.0	69.8	89.6	99.7	100
North-eastern 4120 m	22169	14.9	93.6	98.6	99.9	100
North-eastern 4430 m	9176	17.1	89.8	97.9	100.0	100

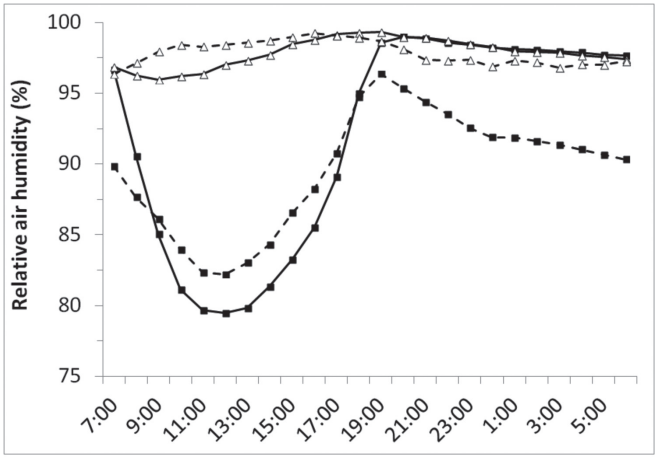

FIG. 10 - Daily course of relative air humidity at 100 cm above ground at the western lower (squares and solid curve), western higher (squares and dashed curve), north-eastern lower (triangles and solid curve), and north-eastern higher (triangles and dashed curve) climatic stations.

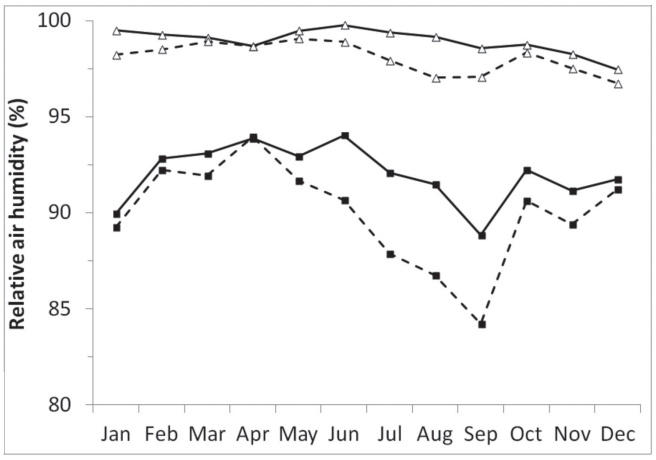

FIG. 11 - Seasonal course of mean daily relative air humidity at 100 cm above ground at the western lower (squares and solid curve), western higher (squares and dashed curve), north-eastern lower (triangles and solid curve), and north-eastern higher (triangles and dashed curve) climatic stations.

lower site during the entire night, RH culminated after the sunset at ~96% at the western higher site and then declined gradually to 90% in the morning. As regards the seasonal variation, mean daily RH peaked at ~94% at both western sites in April but dropped in September to 89% and to 84% at the lower and higher sites respectively.

POTENTIAL EVAPOTRANSPIRATION

Differences in solar radiation, air temperature, and relative air humidity between the opposite sides of the Antisana volcano resulted in the potential evapotranspiration (Et_o) at the north-eastern sites being only 70% of that estimated for the western sites (tab. 4). On the other hand, due to minor differences in the incoming radiation and relative air humidity between the lower and higher sites, there was only a minor difference in Et_o due to elevation. Cumulative values of Et_o and precipitation for the one-year period of December 2009–November 2010 (for which a complete dataset was available) were, respectively, 732 mm and 1455 mm for the western lower site. A modest water balance deficit developed there during December–March due to lower precipitation and slightly higher Et_o (fig. 12). The cumulative values of Et_o and precipitation were, respectively, 515 mm and 2626 mm for the north-eastern side with precipitation exceeding evaporative demands during the entire year. The seasonal variation in Et_o was 16.9% at the western lower site and 11.6% at the north-eastern lower site.

TABLE 4 - Means and extreme values of potential evapotranspiration Et_0.

Station	Minimum (mm day^{-1})	Mean (mm day^{-1})	Maximum (mm day^{-1})
Western 4280 m	0.8	2.0	4.0
Western 4600 m	0.6	2.1	4.0
North-eastern 4120 m	0.6	1.4	4.2
North-eastern 4430 m	0.5	1.4	3.3

DISCUSSION

Three years of observations is too short a period to provide a complete picture of temporal climate variation in the equatorial high Andes (Francou & *alii*, 2004). Nevertheless, the annual and inter-annual variation patterns documented by our measurements on the western side of the Antisana volcano are fully consistent with those observed in the vicinity of the Antisana glacier on the same mountain side during 2007–2010 (e.g., Rabatel & *alii*, 2013), which supports the validity of our data. During our measurements, the ENSO index was negative except for May-2009–May-2010 when it turned positive; in fact, one of the strongest El Niño/La Niña oscillations over the past few decades occurred between 2009 and 2011 (e.g. Boening & *alii*, 2012). The ENSO is imprinted in the inter-annual variation of all measured variables and particularly so on the western side of the mountain (fig. 13). Relative air humidity and precipitation tend to correlate negatively whereas global radiation tends to correlate positively to ENSO. These correlations became stronger with the onset of the 2009 El Niño event. However, since less cloud cover during an El Niño event not only reduces precipitation in the Andes but it also increases air temperature (Francou & *alii*, 2004; Vuille & *alii*, 2008), the negative correlation of air temperature with ENSO in the first part of the measurements turned strongly positive since mid-2009 on both sides of the mountain. Our observations thus covered the variation between "standard" years and a strong El Niño/La Niña event which allows for describing major climatic trends that occur in the high-elevation páramo of Antisana.

Heavy convective clouds from the Amazon basin are lifted by the Andean cordillera and bring plentiful rainfall

to the eastern slopes of the Ecuadorian Andes (Bendix & Lauer, 1992; Vuille & *alii*, 2000a; Bendix & Rafiqpoor, 2001; Favier & *alii*, 2004; Laraque & *alii*, 2007). The precipitation increases from 1434 mm in the montane forest (Papallacta, 3160 m; Bendix & Rafiqpoor, 2001) to 2694 mm on the north-eastern side of the Antisana volcano (4100 m). Such an amount ranks this páramo among the most humid in Ecuador (Jorgensen & Ulloa, 1994) and by the temporal rainfall pattern makes it similar to the eastern slope of the Sumapaz páramo in the Colombian eastern cordillera (Las Dantas, 3996 m, annual sum of 5445 mm with a distinct maximum in June–July; Rangel & Arellano, 2008). The clouds flow around the cone of the volcano, which often leaves its western slope without rain or even sunlight. This leeward side of the mountain thus receives 2–4 times less rain than the opposite, windward side. While a significant portion of precipitation in the eastern cordillera originates from humidity that is advected from the Quito basin (Bendix & Rafiqpoor, 2001; Lauer & *alii*, 2001), the western (leeward) side of the Antisana volcano has two rainy periods (see also Villacís, 2008) corresponding to the general precipitation pattern of the Ecuadorian inter-Andean valley. This is similar to the western side of Sumapaz (Laguna Chisaca, 3800 m, 1245 mm) and páramo Los Nevados in the Colombian central cordillera (precipitation sums between 1200–1500 mm) (Bendix & Lauer, 1992; van der Hammen & *alii*, 1995; Bendix & Rafiqpoor, 2001; Laraque & *alii*, 2007; Rangel & Arellano, 2008; IAEA, 2009). Moreover, contrary to the eastern side, rainfall declines with elevation from 1607 mm observed at the climatic station Pinantura (3250 m) to about 1100 mm measured in this study (4280 m) and 977 mm observed at 4700 m (Villacís, 2008). Nevertheless, precipitation tends to increase again in the vicinity of the glacier (4860 m) as suggested by reports of annual sums above 1000 mm (Favier & *alii*, 2004, 2008; Maisincho & Carceres, 2007; Wagnon & *alii*, 2009).

Such contrasting precipitation patterns determine the spatial climatic variation observed on the Antisana volcano. Solar radiation input is almost 1.6 times greater on the western (leeward) side of the mountain and peaks in July–September, i.e., during the period of reduced cloudiness and rainfall (Favier & *alii*, 2004; Wagnon & *alii*, 2009). There is a seasonal decline of relative air humidity to mean values below 90% during the driest month (September), as well as a distinct mid-day minimum, which is consistent with patterns observed in the Colombian (central cordillera) and Venezuelan páramos, although the RH values are lower there (Azócar & Monasterio, 1980; Witte, 1995). The nightly decline of RH at the western higher site is similar to the Venezuelan Páramo de Mucubají (Azócar & Monasterio, 1980) and may be due to the down-flow of cold and relatively dry air (RH ~78%) from the Antisana glacier (Wagnon & *alii*, 2009). Evaporative demand is relatively high on the western side and a modest deficit in water supply may develop temporarily during periods of reduced rainfall in December–March, similar to the seasonal Páramo de Mucubají, although the water deficit during the driest month is much higher there (Azócar & Monasterio, 1980). The vigorous advective regime on the eastern (windward) side of

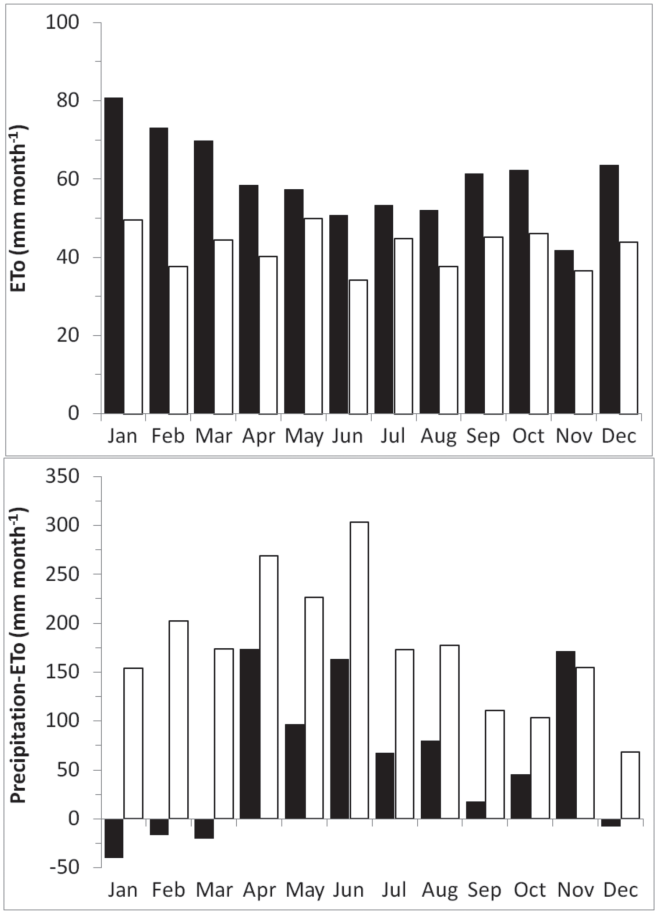

FIG. 12 - Monthly sums of potential evapotranspiration ET_0 (above) and difference between precipitation and ET_0 (below) for the western (black columns) and north-eastern (white columns) sides during December 2009–November 2010.

Antisana brings atmospheric moisture which eliminates any daily or seasonal pattern in relative air humidity, consistent with the climate at Papallacta (Bendix & Rafiqpoor, 2001). Heavy clouds, along with high relative air humidity and frequent fogs, produce very low evapotranspiration values, which are comparable to the humid grass páramo of southern Ecuador and to Sumapaz in Colombia (Buytaert & *alii*, 2007; Rangel & Arellano, 2008).

The lack of thermal seasonality is the most obvious feature of the tropical alpine and montane climates (e.g., Hedberg, 1964; Sarmiento, 1986; Rundel, 1994; Bendix & Rafiqpoor, 2001). This is confirmed by our measurements in the high-elevation páramo of Antisana although we also document distinct variation in this general pattern. For instance, the diurnal variation of air temperature is more than seven times greater than the annual variation on the western side of the mountain (tab. 5). Due to permanently high humidity on the opposite north-eastern side, however, daily temperature oscillation is much more limited, which reduces the ratio of daily/annual variation to 2–2.4, i.e., values which are below the common range reported for

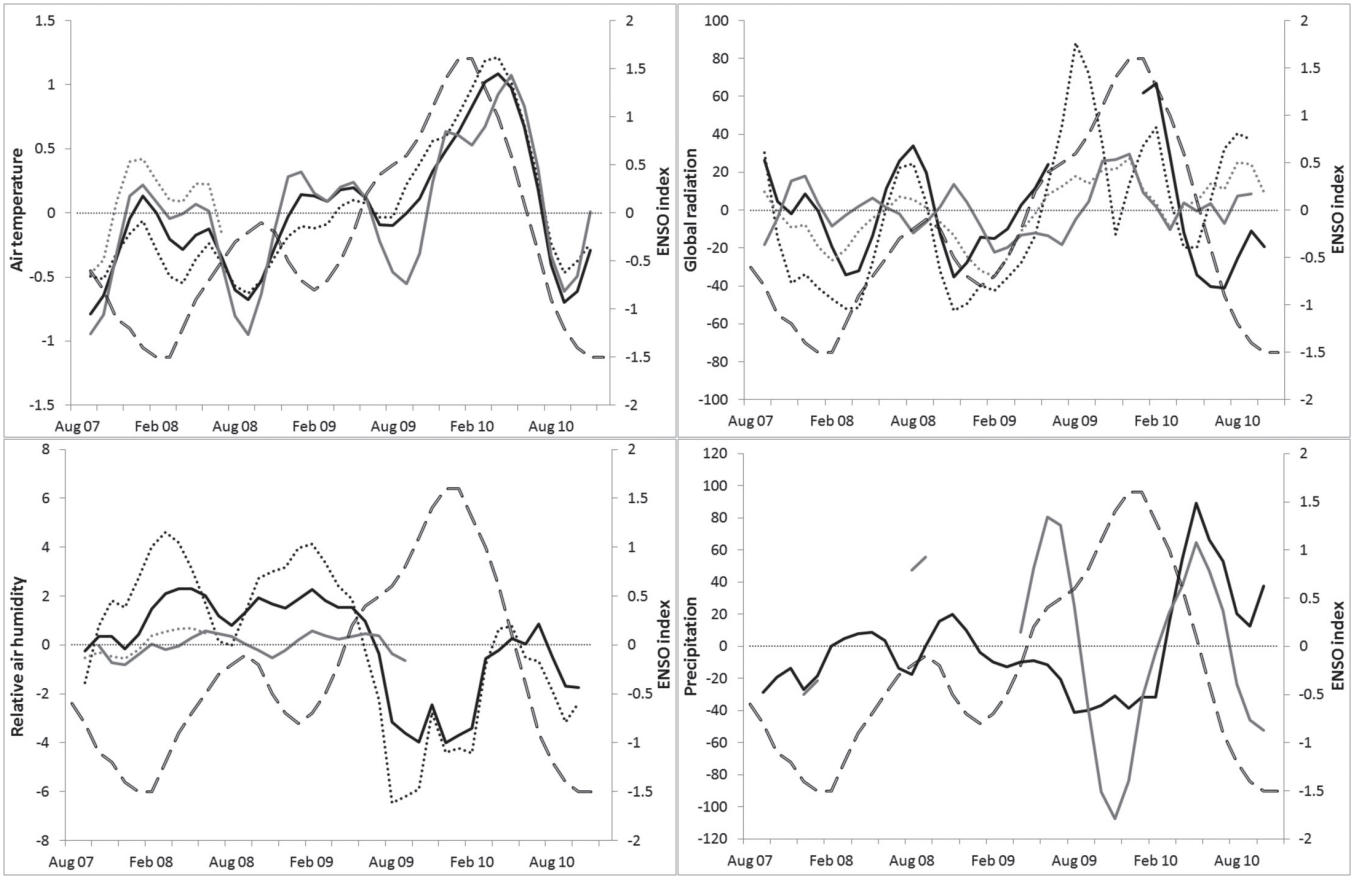

FIG. 13 - Temporal variation of measured climatic variables and their correlation to the ENSO index. Each variable has plotted the running means of deviations of monthly means (air temperature, relative air humidity, global radiation) or monthly sums (precipitation) from the grand mean (e.g., air temperature and relative air humidity in Tables 2, 3), consistently with the ENSO index provided by NOAA (http://www.cpc.noaa.gov/products/analysis_monitoring/ensostuff/ensoyears.shtml; accessed at March 2015); solid black – WL, dotted black – WH, solid gray – EL, dotted gray – EH, dashed double line – ENSO index.

tropical alpine environments (Rundel, 1994). The absolute seasonal minimum, along with the mean daily minimum, exhibits the greatest relative variation during the year, consistent with observations from the Venezuelan páramos (Sarmiento, 1986).

There is no consistent difference between the two mountain sides in terms of daily vs. seasonal relative variation of solar radiation (tab. 5). This is mainly due to the fact that the occurrence of clouds on the eastern side of the Antisana volcano reduces not only the daily radiation input but also its seasonal variation. Air humidity is permanently high on the north-eastern side, so there is virtually neither daily nor annual RH variation. At the western lower site, however, the daily variation of RH is more than five times greater than the annual variation (tab. 5). Since air humidity at the western higher site varies both diurnally and annually, the daily variation relative to the seasonal one is comparable to the north-eastern mountain side.

TABLE 5 - Ratio of daily to monthly variation of climatic variables at the four climatic stations.

	Air temperature	Solar radiation	Relative air humidity
Western 4280 m	7.1	7	5.2
Western 4600 m	7.3	4.8	1.6
North-eastern 4120 m	2	5.8	1.7
North-eastern 4430 m	2.4	6.4	1.1

Night frost may occur anytime during the year in the tropical high mountains, but particularly during periods of reduced rainfall (Azócar & Monasterio, 1980; Sarmiento, 1986). This pattern is confirmed in the Antisana páramo as the occurrence of freezing temperatures has a distinct seasonal pattern and correlates to the dry months. The minimum temperature (–6.1°C) observed during the three years, as well as the rare occurrence of days with mean air temperature below zero, and no day with permanent frost, are all consistent with the environment of the Colombian superpáramo Los Nevados (4500 m, minimum temperature of –8°C) (Witte, 1995; Javellas & Thouret, 1995). Most freezing periods lasted much less than four hours in the páramo

of Antisana, and only rarely continued over the whole night. Thus, although night freezing temperatures are a common and year-round phenomenon in the equatorial páramo, they are mild and of a short duration, at least in the humid regions. Moreover, the nights are becoming warmer since the frequency of the coldest temperatures is decreasing (Vuille & *alii*, 2008). In such thermal conditions, freezing avoidance by, e.g., insulation or transient supercooling, appears to be a convenient strategy for páramo plants and insects to cope with subzero-temperature stress (Beck, 1994; Sømme & *alii*, 1996; Sklenář & *alii*, 2010, 2012).

Since day time temperatures become cooler with increasing elevation, whereas nights remain comparably cold on the western side of the Antisana volcano (fig. 7; compare also calculated summed hour-degrees for day and night), the temperature balance is largely driven by radiation during the day rather than heat loss during the night. The mean annual air temperature thus declines from 3.7°C to 2.3°C between the western sites giving a temperature lapse rate of 0.44 K/100 m. This lapse rate (0.46 K/100 m) stays consistent in the upper reaches of the páramo belt since the mean annual temperature is 1.1°C in the vicinity of the glacier (4860 m) on the western side of the mountain (Wagnon & *alii*, 2009). The north-eastern side of the Antisana volcano is different as both the day and night mean temperatures decrease with elevation. The mean annual air temperature declines from 3.8°C to 2.1°C giving a lapse rate of 0.55 K/100 m. The lapse rates estimated for the high-elevation páramo belt are quite consistent with the values of 0.43 K and 0.50 K per 100 m provided by Cañadas Cruz (1983; cited in Jørgensen & Ulloa, 1994) for the western and eastern slopes of the Ecuadorian Andes, respectively. On the other hand, our values are lower than the lapse rate of 0.59 K/100 m reported for the 2000–4500 m elevational gradient in the Colombian Los Nevados (Javellas & Thouret, 1995).

Due to its location virtually at the Equator, the annual variation of mean air temperature is less than 2K in the páramo belt, which is consistent with observations from the Antisana glacier foreland (Villacís, 2008). In this regard, the thermal conditions are indeed aseasonal with important inter-annual variation due to the ENSO events (Francou & *alii*, 2004; Rabatel & *alii*, 2013). However, distinct seasonal variation exists with regards to precipitation, to which variations in solar radiation, frequency of frosts, temperature extremes, relative air humidity, and evapotranspiration are correlated. The climatic variation is more pronounced on the western side of the mountain, which thus experiences greater extremes than the north-eastern mountain side. Reduced cloud frequency on the western side, along with lower precipitation, results in higher radiation, higher air temperatures, and lower relative air humidity during the day. Water availability to páramo plants may be occasionally limited during drier periods, especially in poorly developed soils or rocky outcrops (e.g., Pfitsch, 1994). In contrast, high rainfall, in combination with low air temperatures and high air humidity, reduces potential evapotranspiration, thus there is always surplus of water on the eastern side of the Antisana volcano. Therefore, the eastern side of the mountain has very high water yield connected with a steadily high water discharge. Such climatic variation between the opposite sides of the Antisana volcano is reflected by the distinct species composition and community structure of the páramo vegetation (Sklenář & Lægaard, 2003) as well as by variation in the ^{13}C stable isotope signal in plant tissues (Macková & *alii*, unpublished data).

References

Anonymous. (1978–1990) *Anuario Meteorológico*. Instituto Nacional de Meteorología e Hidrología. Ministerio de energia y Minas, Quito.

Allen R.G., Pereira L.S., Raes D. & Smith M. (1998) - *Crop evapotranspiration - Guidelines for computing crop water requirements* - FAO Irrigation and drainage paper 56, FAO - Food and Agriculture Organization of the United Nations, Rome. http://www.fao.org/docrep/X0490E/x0490e00.htm#Contents

Azócar A. & Monasterio M. (1980) - *Caracterización ecológica del clima en el Páramo de Mucubají*. In: Monasterio, M. (Ed.): "Estudios ecológicos en los páramos andinos". Editorial de la Universidad de los Andes, Mérida, 207–223.

Barry R.G. (2008) - *Mountain Weather and Climate*. 3rd Ed. Cambridge.

Beck E. (1994) - *Cold tolerance in tropical alpine plants*. In: Rundel P.W., Smith A.P. & Meinzer F.C. (Eds.), "Tropical Alpine Environments. Plant Form and Function". Cambridge, 77–110.

Bendix J. & Lauer W. (1992) - *Die Niederschlagsjahreszeiten in Ecuador und ihre klimadynamische Interpretation*. Erdkunde, 46, 118–134.

Bendix J. & Rafiqpoor M.D. (2001) - *Studies on the thermal conditions of soils at the upper tree line in the páramo of Papallacta (Eastern Cordillera of Ecuador)*. Erdkunde, 55, 257–276.

Black J.M. (1982) - *Los páramos del Antisana*. Revista Geográfica, 17, 25–52.

Boening C., Willis J.K., Landerer F.W., Nerem S.R. & Fasullo J. (2012) - *The 2011 La Niña: So strong, the oceans fell*. Geophysical Research Letters, 39, L19602, doi:10.1029/2012GL053055.

Buytaert W., Iniguez V. & de Bièvre B. (2007) - *The effects of afforestation and cultivation on water yield in the andean páramo*. Forest Ecology and Management, 251, 22–30.

Cañadas Cruz L. (1983) - *El mapa bioclimático y ecológico del Ecuador*. Quito.

Clapperton C.M., Hall M., Mothes P., Hole M.J., Still J.W., Helmens K.F., Kuhry P., & Gemmell A.M.D. (1997) - *A Younger Dryas icecap in the equatorial Andes*. Quaternary Research, 47, 13–28.

Diemer M. (1996) - *Microclimatic convergence of high-elevation tropical páramo and temperate-zone alpine environments*. Journal of Vegetation Science, 7, 821–830.

Fagua J.C. & Gonzalez V. H. (2007) - *Growth rates, reproductive phenology, and pollination ecology of* Espeletia grandiflora *(Asteraceae), a giant Andean caulescent rosette*. Plant Biology, 9, 127–135.

Favier V., Wagnon P., Charazin J.P., Maisincho L. & Coudrain A. (2004) - *One-year measurements of surface heat budget on the ablation zone of Antizana Glacier 15, Ecuadorian Andes*. Journal of Geophysical Research, 109, D18105, doi:10.1029/2003JD004359.

Favier V., Coudrain A., Cadier E., Francou B., Ayabaca E., Maisincho L., Pradeiro E., Villacis M. & Wagnon P. (2008) - *Evidence of groundwater flow on Antizana ice-covered volcano, Ecuador*. Hydrological Sciences Journal, 53, 278–291.

Francou B., Vuille M., Favier V. & Cáceres B. (2004) - *New evidence for an ENSO impact on low-latitude glaciers: Antizana 15, Andes of Ecuador, 0°28'S*. Journal of Geophysical Research 109: D18106, doi:10.1029/2003JD004484

Grubb P.J. (1970) - *The impact of man on the Páramo of Cerro Antisana*. Journal of Applied Ecology, 7, 7-8.

Hall M. (1977) - *El Volcanismo en el Ecuador*. Quito.

Hastenrath S. (1981) - *The Glaciation of the Ecuadorian Andes*. Rotterdam.

Hedberg O. (1964) - *Features of Afroalpine plant ecology*. Acta Phytogeographica Suecica, 49, 1-144.

IAEA (2009) - *Atlas of isotope hydrology - the Americas*. International Atomic Energy Agency, Vienna.

Javellas R. & Thouret J.C. (1995) - *Estudio de las temperaturas de las estaciones meteorologicas del transecto Parque Los Nevados (Cordillera Central, Colombia).* In: van der Hammen T. & Dos Santos A.G. (Eds.), "La Cordillera Central Colombiana. Transecto Parque Los Nevados". Studies on Tropical Andean Ecosystems 4. Berlin, 241-278.

Jomelli V., Favier V., Rabatel A., Brunstein D., Hoffmann G. & Francou B. (2009) - *Fluctuations of glaciers in the tropical Andes over the last millennium and palaeoclimatic implications: A review*. Palaeogeography, Palaeoclimatology, Palaeoecology, 281, 269-282

Jørgensen P.M. & Ulloa C.U. (1994) - *Seed plants of the high Andes of Ecuador - a checklist*. AAU Reports, 34, 1-443.

Kudo G. & Suzuki S. (2004) - *Flowering phenology of tropical-alpine dwarf trees on Mount Kinabalu, Borneo*. Journal of Tropical Ecology, 20, 563-571.

Laraque A., Ronchail J., Cochonneau G., Pombosa R. & Guyot J.L. (2007) - *Heterogeneous distribution of rainfall and discharge regimes in the Ecuadorian Amazon Basin*. Journal of Hydrometeorology, 8, 1364-1381.

Lauer W. (1979) - *Die hypsometrische Asymmetrie der Páramo Höhenstufe in den nördlichen Anden*. Innsbrucker Geografische Studien, 5, 115-130.

Lauer W., Rafiqpoor M.D. & Thiesen I. (2001) - *Physiogeohrapgie, Vegetation und Syntaxonomie der Flora des Páramo de Papallacta (Ostkordillere Ecuador)*. Erdwischenschaftliche Forschung 39. Stuttgart.

Maisincho L. & Caceres B. (2007) - *Glaciares del Ecuador: Antisana y Carihuayrazo*. IRD – INAMHI – EMAAP-Quito, Quito.

NOAA (2015) - http://www.cpc.noaa.gov/products/analysis_monitoring/ensostuff/ensoyears.shtml.

Pfitsch W.A. (1994) - *Morphological and physiological radiation in páramo* Draba. In: Rundel P.W., Smith A.P. & Meinzer F.C. (Eds.), "Tropical Alpine Environments. Plant Form and Function". Cambridge, 151-165.

Rabatel A. & *alii* (2013) - *Current state of glaciers in the tropical Andes: a multi-century perspective on glacier evolution and climate change*. The Cryosphere, 7, 81-102.

Rangel J.O. & Arellano H. (2008) - *El clima en el área del transecto Sumapaz (cordillera Oriental)*. In: van der Hammen T. (Ed.), "La Cordillera Oriental Colombiana. Transecto Sumapaz". Studies on Tropical Andean Ecosystems 7. Berlin, 143-184.

Rundel P.W. (1994) - *Tropical alpine climates*. In: Rundel P. W., Smith A. P. & Meinzer F. C. (Eds.), "Tropical Alpine Environments. Plant Form and Function". Cambridge, 21-44.

Sarmiento G. (1986) - *Ecological features of climates in high tropical mountains*. In: Vuilleumier F. & Monasterio M. (Eds.), "High Altitude Tropical Biogeography". Oxford, 11-45.

Sauer W. (1971) - *Geologie von Ecuador*. Berlin.

Sklenář P. (1999) - *Nodding capitula in superpáramo Asteraceae: An adaptation to unpredictable environment*. Biotropica, 31, 394-402.

Sklenář P. (2000) - *Vegetation Ecology and Phytogeography of Ecuadorian Superpáramos*. Ph.D. dissertation, Charles University, Prague.

Sklenář P. (2006) - *Searching for altitudinal zonation: species distribution and vegetation composition in the superpáramo of Volcán Iliniza, Ecuador*. Plant Ecology, 184, 337-350.

Sklenář P., Bendix J. & Balslev H. (2008) - *Cloud frequency correlates to plant species composition in the high Andes of Ecuador*. Basic and Applied Ecology, 9, 504-513.

Sklenář P., Kučerová A., Macek P. & Macková J. (2010) - *Does plant height determine the freezing resistance in the páramo plants?* Austral Ecology, 35, 929-934.

Sklenář P., Kučerová A., Macek P. & Macková J. (2012) - *The frost resistance mechanism in neotropical alpine plants is related to geographic origin.* New Zealand Journal of Botany, 50, 391-400.

Sklenář P. & Lægaard S. (2003) - *Rain-shadow in the high Andes of Ecuador evidenced by páramo vegetation.* Arctic Antarctic and Alpine Research, 35, 8-17.

Sømme L., Davidson R.L. & Onore G. (1996) - *Adaptation of insects at high altitudes of Chimborazo, Ecuador*. European Journal of Entomology, 93, 313-318.

Troll C. (1968) - *The cordilleras of the tropical Americas. Aspects of climatic, phytogeographical and agrarian ecology.* In: Troll C. (Ed.), "Geoecology of the tropical mountainous regions of the tropical Americas". Colloquium Geographicum 9. Bonn, 15-56.

Van der Hammen T., Witte H.J.L. & van Reenen G.B.A. (1995) - *Aspectos ecoclimáticos del area del transecto Parque Los Nevados.* In: Van der Hammen T. & Dos Santos A.G. (Eds.), "La Cordillera Central Colombiana. Transecto Parque Los Nevados". Studies on Tropical Andean Ecosystems 4. Berlin, 329-364.

Villacís M. (2008) - *Ressouces en eau glaciaire dans les Andes d'Equateur en relation avec les variations du climat: Le cas du volcan Antisana.* Ph.D. Thesis, Université Montpellier II.

Vuille M., Bradley R.S. & Keimig F. (2000a) - *Climate variability in the Andes of Ecuador and it relation to tropical Pacific and Atlantic sea surface temperature anomalies.* Journal of Climate, 13, 2520-2535.

Vuille M., Bradley R.S. & Keimig F. (2000b) - *Interannual climate variability in the Central Andes and its relation to tropical Pacific and Atlantic forcing.* Journal of Geophysical Research, 105, 12447-12460.

Vuille M., Francou B., Wagnon P., Juen I., Kaser G., Mark B.G. & Bradley R.S. (2008) - *Climate change and tropical Andean glaciers: Part, present and future.* Earth-Science Reviews, 89, 79-96.

Wagnon P., Lafaysse M., Lejeune Y., Maisincho L., Rojas M. & Chazarin J.P. (2009) - *Understanding and modeling the physical processes that govern the melting of snow cover in a tropical mountain environment in Ecuador.* Journal of Geophysical Research, 114, 1-14.

Witte H.J.L. (1995) - *Seasonal and altitudinal distribution of precipitation, temperature and humidity in the Parque Los Nevados transect (Central Cordillera, Colombia).* In: van der Hammen T. & Dos Santos A.G. (Eds.), "La Cordillera Central Colombiana. Transecto Parque Los Nevados". Studies on Tropical Andean Ecosystems 4. Berlin, 279-328.

(*Ms. received 30 August 2014; accepted 1 February 2015*)